Internal Identifier: Deliverable D6.3

Guidelines about properties of AM parts produced by steel S and steel T

10 June 2021

KAVA Reference (Number, Acronym, Full Title):
17070, SPAcEMAN, Sustainable Powders for AdditivE MANufacturing

Name of the authors: M. Abdelwahed, F. Gili, S. Petrella, M. Vedani, C. Wilsnack
Responsible partner: HOG - Höganäs

Version No: 1

This activity has received funding from the European Institute of Innovation and Technology (EIT), a body of the European Union, under the Horizon 2020, the EU Framework Programme for Research and Innovation

Content

This activity has received funding from the European Institute of Innovation and Technology (EIT), a body of the European Union, under the Horizon 2020, the EU Framework Programme for Research and Innovation

1. Introduction

After a wide screening of different steel grades for structural (S-type) and tooling (T-type) applications carried out in the first stage of the project, investigations have been focussed on the two selected grades: the water atomized SPM13 S-steel and the gas atomized SPM 11-2 T-steel.

In this report data are collected about the performance of the two steels. Additional information is also provided by a literature review, aimed at widening the database of mechanical properties available for the design by additive manufacturing of mechanical parts. Due to its potential applications, most of the data are focussed on the S-type steel. As for the T-type steel, also developed within the SPAcEMAN project, information more focussed on laser metal deposition (LMD) manufacturing issues, is provided.

This activity has received funding from the European Institute of Innovation and Technology (EIT), a body of the European Union, under the Horizon 2020, the EU Framework Programme for Research and Innovation

2. Selection of the reference steels

2.1. S-type steel for LPBF

Considering the achieved results and the perspective applications, for the S-type alloys, the main interest was be focussed on the SPM13 alloy, which is to be considered as the newly developed version of the already existing gas atomized (GA) X-4130 steel grade, with a modified composition that makes it more suitable to water atomization (WA).

Motivation for alloy selection

The GA type X-4130 alloy (nominal composition Fe-0.3C-1Cr-0.25Mo-0.6Mn-0.3Si) shows the following advantages considering the powder production aspects:

- Atomization is not very sensitive to composition within the selected range
- Printing of powder with carbon in the higher range is possible without cracking
- Carbon level can possibly be adjusted in order to reach sufficient hardness

The WA type SPM13 alloy (Nominal composition Fe-0.3C-1Cr-0.25Mo-0.1Mn-0.3Si) features the following characteristics:

- The powder after WA features irregular morphology, higher oxygen content and cannot be alloyed with Mn.
- The packing density will be lower, which may influence process robustness and productivity negatively. However, the packing density can be improved by post treatment and using a wider particle size distribution.
- Possibly, it will be beneficial to increase Cr content and C content in order to reach desired hardness.

Two heat treatments are possible for this material: tempering directly after printing, to stabilize the martensite and relieve residual stresses, or a conventional quench and temper process. For cost saving, the use of the steel in as built condition could in principle also be evaluated.

Composition, manufacturing details, microstructure, hardness

The powder heat composition adopted for the mechanical characterization of the steel and for production of demonstrators is summarized in Table 2.1. For comparison purpose the reference GA X4130 steel was also considered in the testing campaign.

This activity has received funding from the European Institute of Innovation and Technology (EIT), a body of the European Union, under the Horizon 2020, the EU Framework Programme for Research and Innovation

Table 2.1 - Chemical composition (weight %) and processing details of the investigated S-type SPM13 steel powder

Alloy code	C	Cr	Mo	Si	Mn	Ni	O	Process
X4130	0,3	1,0	0,2	0,3	0,6	-	0,05	GA
SPM13	0,3	1,1	0,28	0,45	0,044	-	0,29	WA+ post treatment

Laser powder bed fusion (LPBF) processing of the samples used for final characterization and of the demonstrators was performed using a Concept Laser M2 Cusing system. After process optimization, the parameters given in Table 2.2 were used.

Table 2.2 - LPBF parameters adopted for the fabrication of specimens and demonstrators

LPBF parameter	X-4130	SPM13
Laser power (W)	200	200
Scanning strategy	stripes	stripes
Layer thickness (µm)	40	40
Hatching distance (µm)	90	70
Scanning velocity (mm/s)	500	550
Volume energy density (J/mm^3)	111,1	129,9

The samples were then investigated according to three different thermal treatment schedules, namely:

1. As built
2. As built and tempered @ 550°C for 1hour
3. Annealed @ 840°C for 1 hour, water quenched, tempered @ 550°C for 1hour

Option 2 deserves some further considerations to justify the choice. Figure 2.1 shows the comparative trends of hardness measured for the two investigated S-steels as a function the tempering temperature, starting either from as quenched condition or from as built condition. For both steels the curves of the quenched conditions are initially higher than those of as built condition, but by increasing the tempering temperature the curves tend to overlap, at about 450°C for the SPM13 steel and at 350°C for the X-4139 steel.

It is therefore assumed that the two steels already acquired a partially martensitic structure upon fast cooling from molten state. The martensite thus formed is then partially tempered and residual stresses are relieved with the subsequent adjacent and overlapping laser passes.

This activity has received funding from the European Institute of Innovation and Technology (EIT), a body of the European Union, under the Horizon 2020, the EU Framework Programme for Research and Innovation

Eventually, a condition approximately comparable to that of a conventionally quenching and tempered (Q&T) steel is reached for relatively high tempering temperatures, even without a deliberate annealing, quenching and tempering sequence.

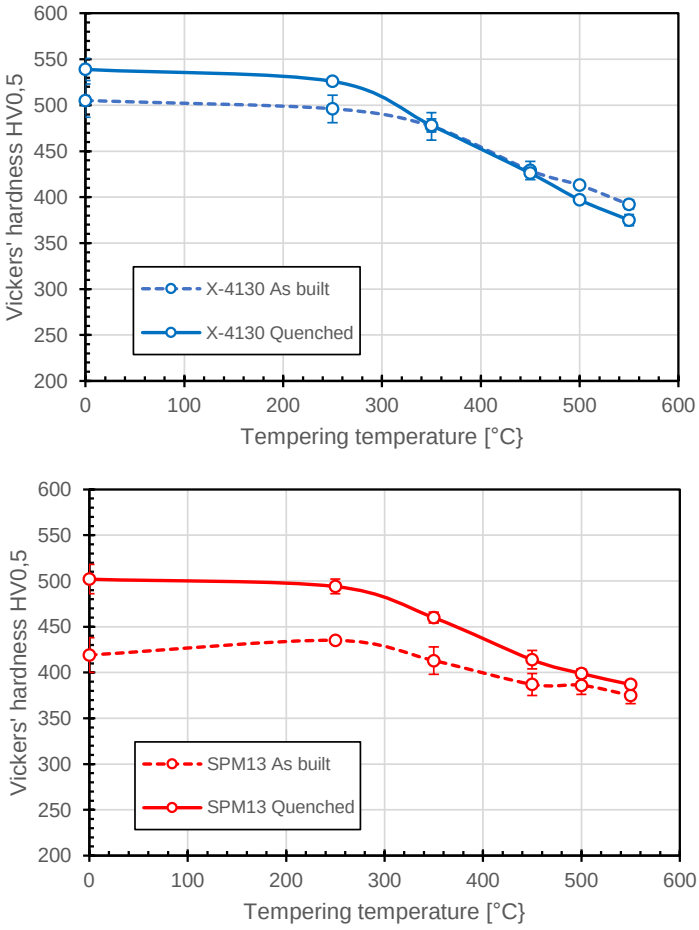

Figure 2.1 – Tempering curves of the investigated steels, starting form as quenched and from as built states

This activity has received funding from the European Institute of Innovation and Technology (EIT), a body of the European Union, under the Horizon 2020, the EU Framework Programme for Research and Innovation

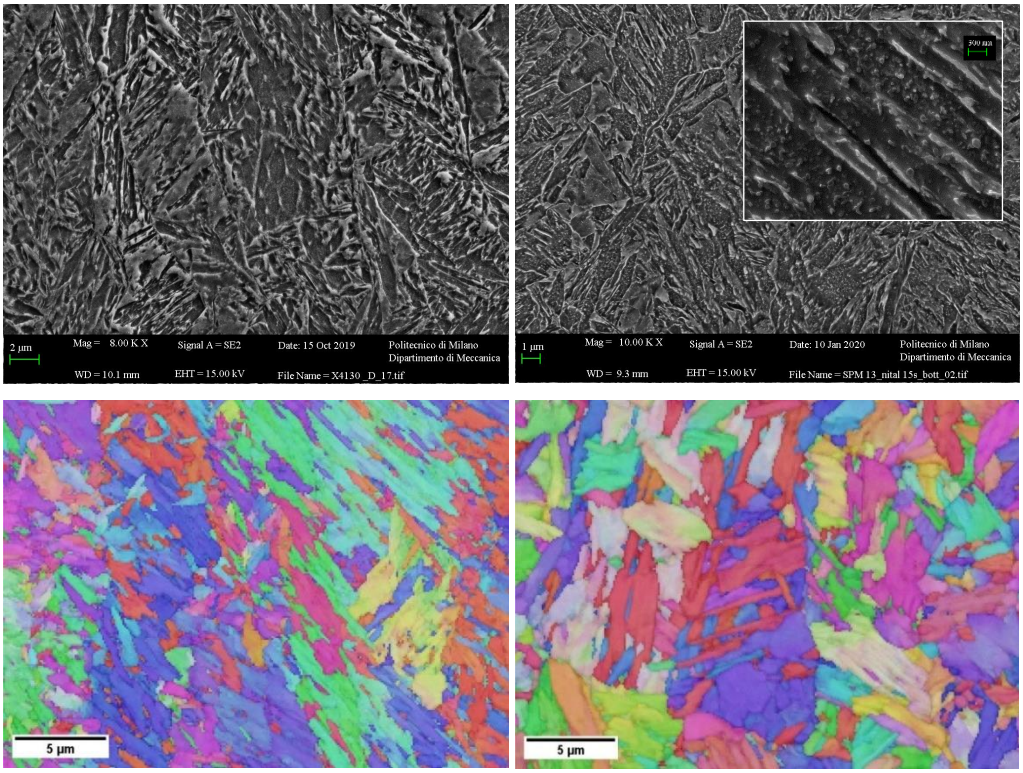

Figure 2.2 – FE-SEM images of the investigated LPBF steels. (a) X-4130 as built, (b) SPM13 as built, and EBSD orientation maps of (c) SPM13 as built, (d) SPM13 as quenched

The achieved microstructures of the steel samples treated according to the selected thermal treatments are given in figure 2.2. A tempered martensite structure is observed in as built samples with minor differences between the steels and the heat treatment condition. Tempered carbides are observed, especially visible in the Inset of Figure (b) taken at higher magnification.

The crystal orientation maps taken by Electron Back Scattered Diffraction (EBSD) reveal the fine martensite plates in the as built SPM13 steel structure (Figure 2.2c) that become coarser in the as quenched state (Figure 2.2d).

2.2. T-type steel for LMD

Motivation for alloy selection

For the intended usage for tooling application to be manufactured by LMD, the T-type SPM11 grade revealed to be very suitable owing to its ability to be processed without generation of hot cracks. As far as powder atomization, the SPM11 steel (nominal composition Fe-0,35C-6Cr-2Mo-

This activity has received funding from the European Institute of Innovation and Technology (EIT), a body of the European Union, under the Horizon 2020, the EU Framework Programme for Research and Innovation

1V -0,7Si-0,2 Mn) is produced by GA due to limitation dictated by its complex composition. The following aspects were considered for its selection:

- Atomization is not very sensitive to composition with the selected range
- The spherical particle shape is beneficial for powder feeding stability
- Processing of powder with a higher Mo-content increases the weldability and leads to a reduction of cracks

Also for the case of the T-type steel, two heat treatment strategies are possible for this material: tempering, directly after printing to stabilize the martensite and relieve residual stresses, or conventional quenching and tempering process.

Composition and manufacturing details

The T-type steel powder heat adopted for the characterization of the steel, especially related to LMD process optimization and for production of the tool demonstrator is given in Table 2.3.

Table 2.3 - Chemical composition (weight %) of the investigated T-type SPM11 steel powder

Alloy code	C	Cr	Mo	Si	Mn	Ni	W	Al	V	Process
SPM11	0,36	6,03	2,06	0,77	0,20	-	-	-	1,01	GA

Specific achievable properties when the steel is LMD processed will strongly depend on processing conditions. In the present case, experiments have been carried out with a DMG Mori Lasertec 65 3D hybrid equipment allowing the combination of additive and subtractive manufacturing with the following properties.

- Adjustable laser spot diameter (1,6 and 3 mm)
- Diode laser, 4 kW laser power
- 4 selectable wave lengths (940-1060 nm)
- Continuous wave laser
- COAX14-V5 powder nozzle, w_d=12 mm
- 5 axis machining

The optimal parameters for the T-steel are given in table 2.4.

Microstructure and hardness

With the above parameters, a sound microstructure could generally be achieved in the deposits, as shown in figures 2.3 and 2.4. The micrographs reveal the presence of columnar grains which grew competitively upon solidification according to thermal gradients. The boundaries of the different melt pools can also be identified in the micrographs but in some cases, cavities can be

This activity has received funding from the European Institute of Innovation and Technology (EIT), a body of the European Union, under the Horizon 2020, the EU Framework Programme for Research and Innovation

detected at their intersections (see figure 2.4). it is believed that these defects could be mitigated by further optimization of the process parameters and adjustment of the deposition strategy.

Table 2.4 - LPBF parameters adopted for the fabrication of specimens and demonstrators

LMD parameter	Value
Laser power (W)	825
Scan rate (mm/min)	750
Powder feed rate (g/min)	8,3
Flow rate Ar carrier gas (l/min)	10
Flow rate Ar shielding gas (l/min)	7
Track width (mm)	1,45
Overlap (%)	30
Track height (mm)	0,8

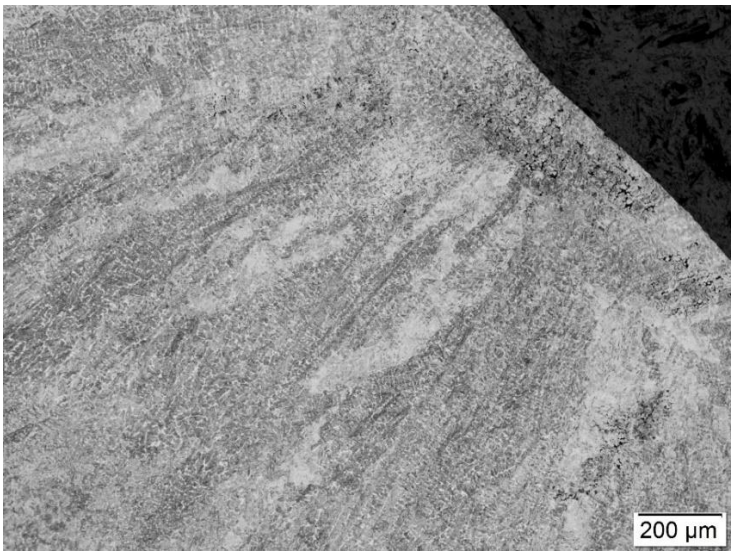

Figure 2.3 – Optical micrograph of a LMD deposit formed with the SPM11 steel

This activity has received funding from the European Institute of Innovation and Technology (EIT), a body of the European Union, under the Horizon 2020, the EU Framework Programme for Research and Innovation

Figure 2.4 – Optical micrograph of a LMD deposit formed with the SPM11 steel showing also cavities formed at track intersections

The LMD steel is usually serviced after a proper thermal treatment which consists in the following sequence:

- Use of a vacuum furnace or inert atmosphere furnace
- Preheating to 850°C with holding time of 60 minutes
- Heating to austenization temperature of 1020°C for 30 minutes
- Quenching in gas or oil, gas is preferred for a more even result and lower risk cracking
- Start tempering directly when the temperature reaches 50-70°C
- Heat to the tempering temperature of 570°C and hold for 60 minutes
- let air cool to room temperature
- Repeat the annealing process at least one time to increase dimensional stability.

Once heat treated, the average hardness measured on a tool sector used as the project demonstrator was in the range 48±2 HRC.

This activity has received funding from the European Institute of Innovation and Technology (EIT), a body of the European Union, under the Horizon 2020, the EU Framework Programme for Research and Innovation

3. Properties of parts

3.1. S-type steel for LPBF

Tensile properties

Tensile tests have been carried out on cylindrical specimens having the geometry given in Figure 3.1, in accordance with ASTM E8/E8M standard. The gauge diameter (D) and length (G) were 9 mm and 45 mm, respectively. Specimens were printed both horizontally and vertically with respect to building direction. Before testing they were machined to remove the rough surface and to achieve the designed size.

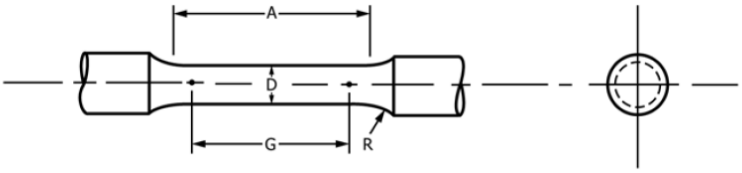

Figure 3.1 – Geometry of the tensile specimens according to ASTM E8/E8M standard

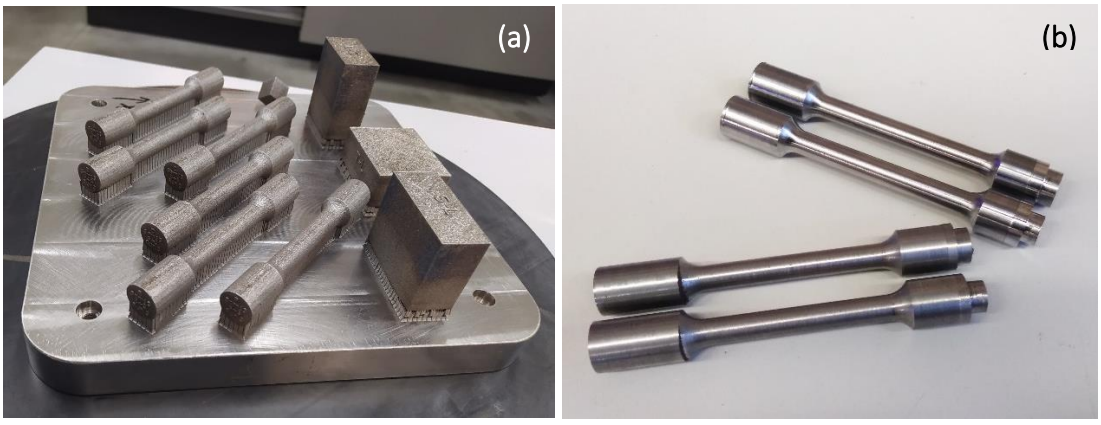

Figure 3.2 – Building platform containing tensile horizontal specimens (a) and view of machined specimens (b)

Tensile tests were carried out at room temperature with an MTS Alliance RT/100 universal testing machine at an initial strain rate of $0.6 \cdot 10^{-3}$ s^{-1}. Three specimens for each condition were generally tested.

This activity has received funding from the European Institute of Innovation and Technology (EIT), a body of the European Union, under the Horizon 2020, the EU Framework Programme for Research and Innovation

A summary of the tensile data obtained from tests is given in Table 3.1, while a general histogram showing the trend of tensile properties is depicted in Figure 3.3.

Table 3.1 – Average tensile properties of the steels investigated (standard deviation of data is given in brackets)

Steel	Orientation	Temper	YS (MPa)	UTS (MPa)	Fracture elong. (%)
X-4130 (GA)	XY	AB	1249 (15)	1419 (30)	3,4 (0,6)
		AB+T	1076 (45)	1127 (58)	2,1 (0,0)
		Q+T	1118 (4)	1170 (10)	6,4 (1,0)
	Z	AB	1166 (5)	1277 (7)	6,3 (0,9)
		AB+T	1057 (11)	1124 (11)	7,9 (1,3)
		Q+T	1125 (1)	1177 (1)	7,9 (0,5)
SPM13 (WA)	XY	AB	1072 (2)	1168 (17)	2,5 (0,1)
		AB+T	1019 (6)	1066 (13)	2,6 (0,3)
		Q+T	1099 (17)	1120 (15)	1,9 (0,1)
	Z	AB	981 (4)	1059 (13)	3,2 (1,5)
		AB+T	952 (8)	1012 (19)	4,2 (2,2)
		Q+T	1110 (10)	1123 (15)	1,4 (0,4)

The tensile data reveal that both steels feature a slight anisotropic behaviour when considering orientation of specimens (XY is for horizontal specimens, having their axis parallel to building plate plane, while Z is for specimens oriented along building direction). The WA SPM13 steel always show slightly lower properties (bot in terms of strength and elongation) with respect to gas atomized X-4130 counterpart. This behaviour can be related to the slight difference in composition (lack of Mn in the SPM13 alloy) and in a larger amount of oxide inclusions found in the water atomized steel.

As far as the effect of thermal treatment is concerned, the tensile data are in full agreement to the hardness curves depicted in Figure 2.1, showing a superior strength of the as built samples and a wider gap for the X-4130 steel between as built and tempered conditions.

This activity has received funding from the European Institute of Innovation and Technology (EIT), a body of the European Union, under the Horizon 2020, the EU Framework Programme for Research and Innovation

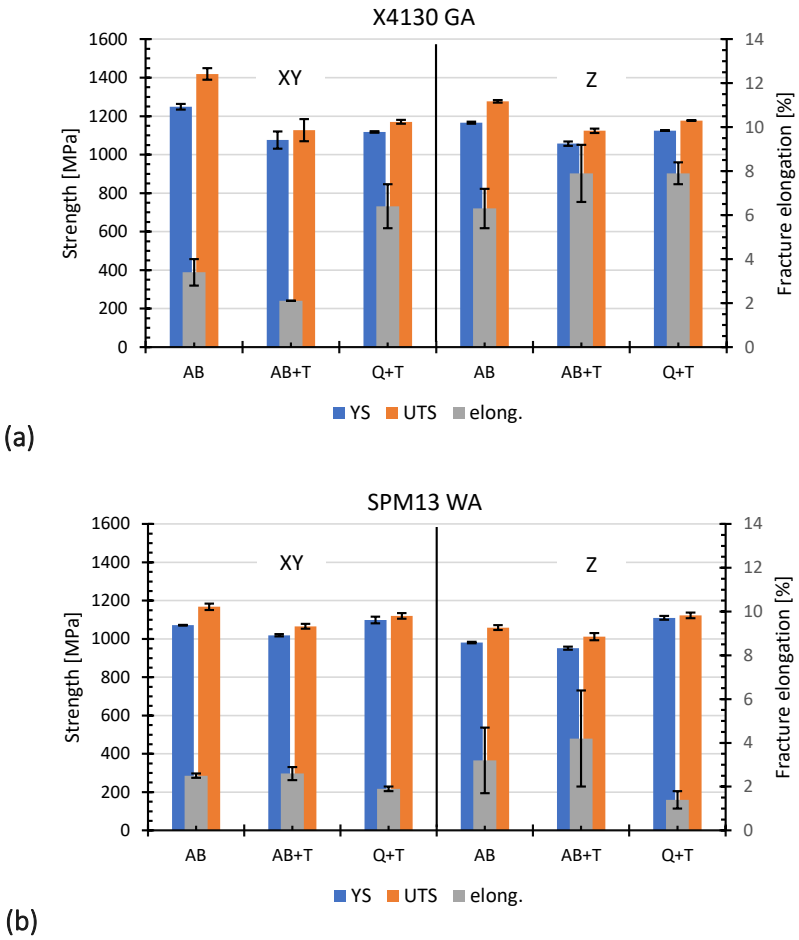

Figure 3.3 – Effect of composition and thermal treatment condition on tensile properties of the steels investigated

The results about the effect of powder recycling on properties of printed parts have been addressed in deliverable D4.2 "Part performance degradation during re-use of powder". The main results have been summarized also here for sake of completeness.

Figure 3.4 reports typical surface features detected on powder particles, showing traces of environmental-gas contamination, already visible on the fresh water-atomized powder after the first exposure in the LPBF chamber, and the presence of large spatters on reused powder.

Data about the chemical composition of powder samples collected after each run are given in Table 3.2. Considering the different runs of the SPM13 WA powder, it can be observed that no significant changes take place during the repeated use of the powder, at least within the conditions and number of runs here considered.

This activity has received funding from the European Institute of Innovation and Technology (EIT), a body of the European Union, under the Horizon 2020, the EU Framework Programme for Research and Innovation

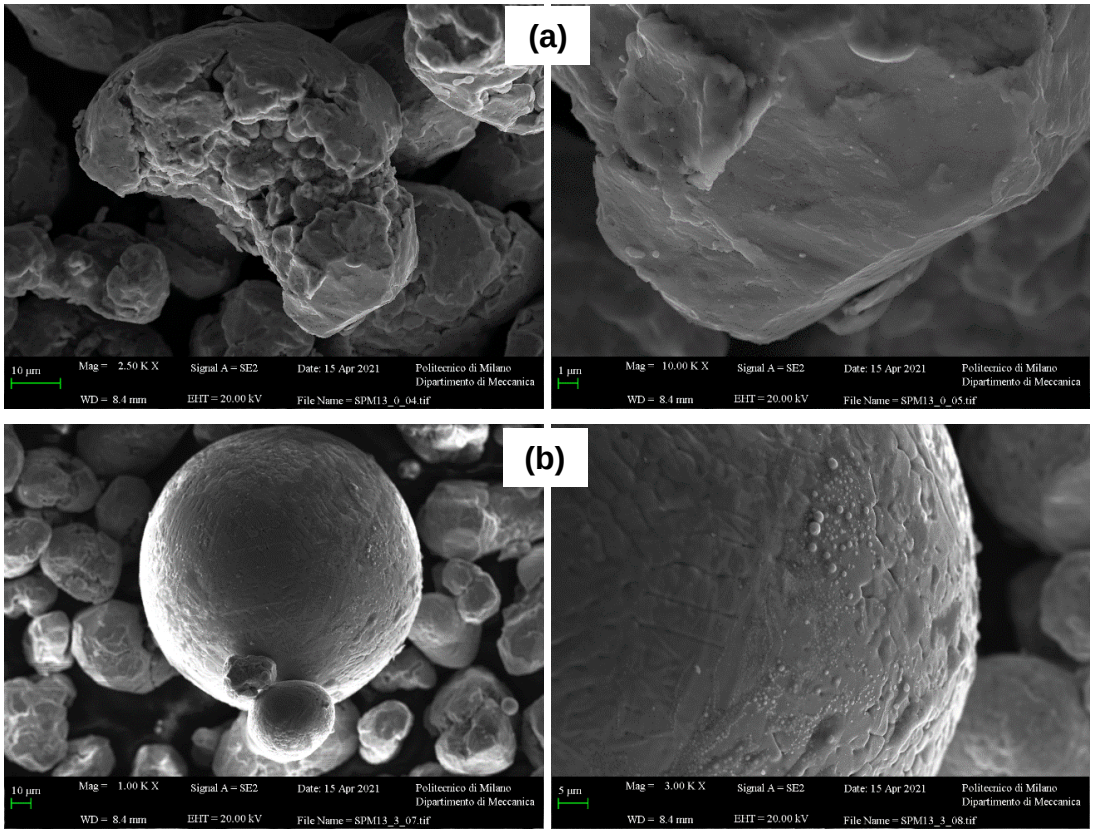

Figure 3.4 – High-magnification views of SPM13 powder particles, (a) run 0, (b) run 3

Table 3.2 – Modification of some selected elements (in weight %) in the investigated powders during recycling tests

Steel & run	C- tot	N	O	S
X-4130 Run 0	0,329	0,0107	0,063	0,008
SPM13 Run 0	0,325	0,0055	0,252	0,015
SPM13 Run 1	0,324	0,0050	0,254	0,015
SPM13 Run 2	0,324	0,0056	0,247	0,015
SPM13 Run 3	0,324	0,0054	0,242	0,015

The change of tensile properties during the different recycling runs is plotted in Figures 3.5. it is shown that tensile properties are not significantly affected by the recycling runs, at least within the experimental conditions and number of recycling runs here explored.

This activity has received funding from the European Institute of Innovation and Technology (EIT), a body of the European Union, under the Horizon 2020, the EU Framework Programme for Research and Innovation

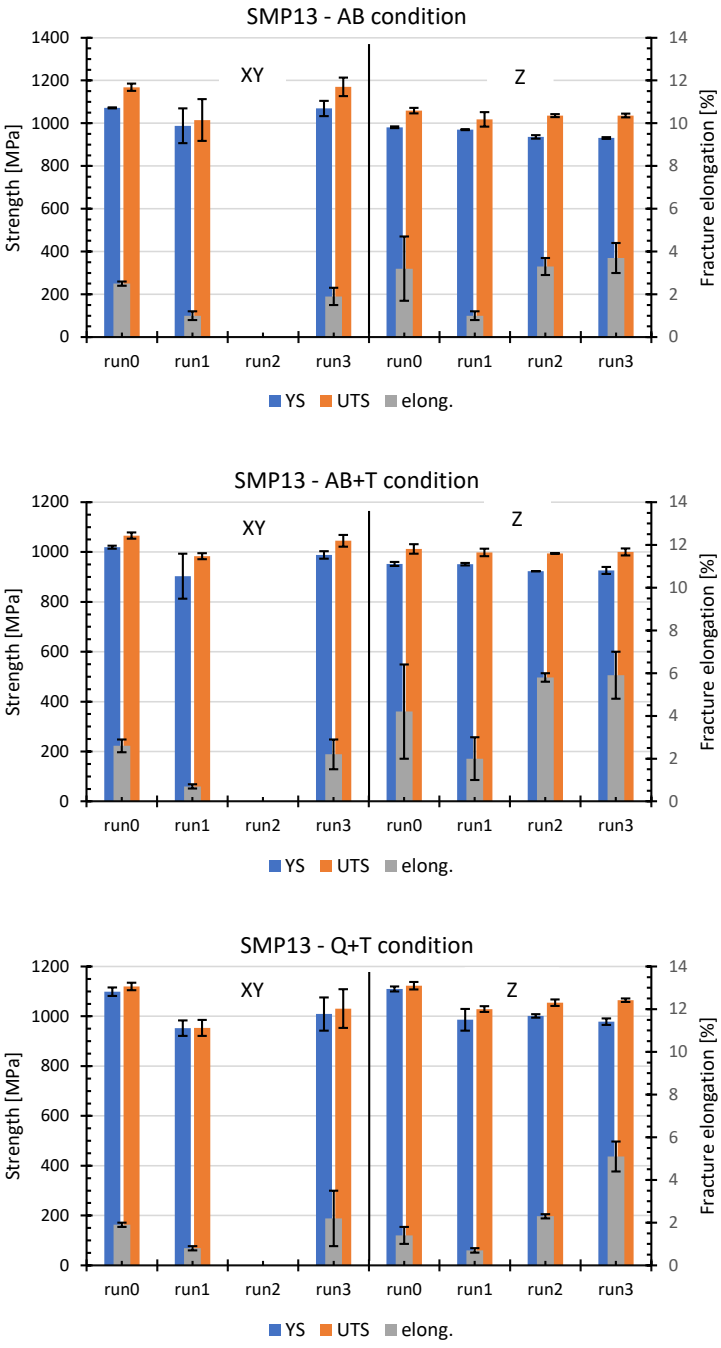

Figure 3.5 – Tensile behaviour of SPM13 WA steels after LPBF, according to indicated number of recycling runs and direction

This activity has received funding from the European Institute of Innovation and Technology (EIT), a body of the European Union, under the Horizon 2020, the EU Framework Programme for Research and Innovation

4. Steel properties from the literature

4.1. Steels for AM

For more scientific details about the steels investigated in the SPAcEMAN project, concerning their constitution and properties, the reader is referred to the published papers [1,2], while issues about powder degradation are addressed in the papers [3,4]. Further general data about properties of steels can be obtained by a number of review papers that have been published in recent times [5-9].

While most of the interest about steels for additive manufacturing is focussed on 304/316L stainless steels and on precipitation hardening (type PH) and Maraging grades, few data are available on ferritic, martensitic, alloy steels and tool steels. For comparison purposes, in Table 4.1 a collection of the tensile properties achievable in austenitic stainless steels is reported [9]. In Tables 4.2 and 4.3 similar data are given for precipitation hardening and maraging steels, respectively. For other structural steels, perhaps of wider interest for more traditional manufacturing routes, but "less-conventional" in additive manufacturing, data are reported in table 4.4 [6].

The data here presented, irrespective of steel grades, highlight the large variability of properties achieved, even for the same nominal steel grade, depending on processing details, chemical composition and heat treatment condition. It is also surprising to see the relatively low number of investigations available on plain Carbon- and alloyed structural steels. An interesting conclusive comment in this respect has been reported by Fayazfar et al. in [6]. It is here integrally reported:

"Last but not least, the number of ferrous alloys deployed to AM processes is extremely limited. While there are >1000 steel alloys for conventional manufacturing (casting, forging, machining, etc.), there have not been many steel alloys deployed to AM by researchers and industry to-date. It becomes a more limiting factor when the number of qualified steel alloys offered by the AM Original Equipment Manufacturers (OEMs) is <10. Further efforts must be made to develop new steel alloys, which are better tailored to AM and also to deploy existing alloys to AM processes, for which imminent market opportunities are expected."

This activity has received funding from the European Institute of Innovation and Technology (EIT), a body of the European Union, under the Horizon 2020, the EU Framework Programme for Research and Innovation

Table 4.1 – Tensile properties of stainless steels fabricated by LPBF [9]

SS alloy	P (W)	v (mm/s)	H (J/mm)	ρ (%)	Orientation	E (GPa)	σ_y (MPa)	σ_{uts} (MPa)	Elongation (%)	HV	Refs.
Directed energy deposition – powder feedstock											
304	–	–	–	100	Long.	–	448	710	59	–	[541]
					Transv.	–	324	655	70	–	
304L	2300	8.5	271	>99.9	Long.	–	337 ± 29	609 ± 18	48.2 ± 2.5	–	[357]
					Transv.	–	314 ± 6	606 ± 13	56.4 ± 5.8	–	
	4000	10.6	371		Long.	–	277 ± 27	581 ± 20	41.8 ± 3.5	–	
					Transv.	–	274 ± 7	560 ± 12	50.5 ± 6.7	–	
316	–	–	–	100	Long.	–	593	807	33	–	[541,675]
					Transv.	–	448	793	36–66	–	
316	–	–	–	93.2–97.4	Long.	192–199	363–487	648–970	20–44		[676]
316	600–1400	2–10	76–500	–	Long.	–	558	639	21	310–350	[472]
					Transv.	–	352	536	46		
316L	570	13	45	99.6	Long.	–	490 ± 8	685 ± 5	51 ± 2	164–215	[677]
					Transv.	–	280 ± 6	580 ± 10	62 ± 5	–	
316L	1000	6	167	–	Long.	–	–	812–901	9–15	305	[482]
316L	400	15	27	100	Long.	–	576	776	33	272 ± 35	[473]
					Transv.	–	479	703	46	289 ± 16	
316L	1650	23.3	71	97.6	Transv.	–	450	510	20	270	[474]
	1450	20	73	96.7	Transv.	–	440	470	18	240	
	1150	16.7	69	96.8	Transv.	–	410	460	22	215	
	1000	13.3	75	96.3	Transv.	–	420	440	15	220	
	800	10	80	96.2	Transv.	–	405	430	14	220	
Powder bed fusion											
304	200	25	8	100	Long.	–	520	710	38	–	[478]
					Transv.	–	450	580	58	–	
304L	95	70	1.36	–	Long.	–	182	393	25.9	217	[660]
		90	1.06	–		–	156	389	22.1	209	
316L	200	Up to 1000	>0.2	99.9	Long.	–	602 ± 47	664 ± 7	30 ± 0	235	[479]
					Transv.	–	557 ± 14	591 ± 12	42 ± 2	–	
316L	100	400	0.25	97.2 ± 1.2	Long.	165	438 ± 28	528 ± 23	10 ± 2	–	[480]
					Transv.	–	435 ± 2	504 ± 12	16 ± 3	–	
		591	0.17	98.5 ± 1.4	Long.	166	379 ± 17	489 ± 28	23 ± 6	–	
					Transv.	–	287 ± 6	317 ± 11	7 ± 4	–	
		600	0.17	98 ± 1.0	Long.	164	399 ± 29	486 ± 40	9 ± 3	–	
					Transv.	–	316 ± 6	367 ± 6	7 ± 1	–	
316L	175	700	0.25	97.5 ± 1	Long.	–	534 ± 5.7	653 ± 3.4	16.2 ± 0.8	–	[475,476]
				93.8 ± 2.6	Transv.	–	444 ± 26.5	567 ± 18.6	8 ± 2.9	–	
316L	380	635–3000	0.13–0.60	>99	–	–	–	–	–	220–213	[469]
316L	100	300	0.33	98.6	–	151.5 ± 13.1	–	501.1 ± 8.3	–	–	[678]
316L	103	425	0.24	–	Transv.	–	640	760	30	–	[481]
Traditionally processed											
304L	Annealed					–	168	556	61	136	[679]
304L	Annealed					–	265 ± 9	722 ± 14	62.3 ± 2.6	–	[357]
316L	Cast					200	365 ± 22	596 ± 16	69 ± 9	–	[480]
316L	Annealed					–	241	586	50	215–225	[473]

P = Laser power, v = Scanning speed, H = Linear heat input, ρ = Density, E = Elastic modulus, σ_y = Yield strength, σ_{uts} = Ultimate tensile strength, HV = Vickers hardness.

Table 4.2 – Tensile properties of PH steels fabricated by LPBF [9]

SS alloy	Post heat treatment	Orientation	σ_y (MPa)	σ_{uts} (MPa)	Elongation (%)	HV	Ref.
17-4 PH	H900 (480 °C for 1 h)	Long.	945 ± 12	1417 ± 6	15.5 ± 1.3	375 ± 3	[485]
	H1025 (550 °C for 4 h)		870 ± 25	1358 ± 8	13.3 ± 1.5	399 ± 8	
	H1150 (620 °C for 4 h)		1005 ± 15	1319 ± 2	11.1 ± 0.4	381 ± 3	
	CA (solution annealed, 1040 °C for 30 min)		939 ± 9	1188 ± 6	9 ± 1.5	330 ± 3	
	CA + H900		1352 ± 18	1444 ± 2	4.6 ± 0.4	417 ± 5	
	CA + H1025		1121 ± 9	1172 ± 2	9.6 ± 1.7	350 ± 4	
	CA + H1150		859 ± 11	1017 ± 15	16.6 ± 1.2	317 ± 3	
17-4 PH	650 °C for 2 h	Transv.	619 ± 1	915 ± 38	12 ± 1	–	[483]
	788 °C for 2 h		857 ± 14	1487 ± 10	7 ± 1	–	
	788 °C for 2 h + H900		1126 ± 14	1457 ± 3	12 ± 3	–	
17-4 PH	CA+H900	Long.	910	1210 ± 10	8 ± 1	–	[487]
		Transv.	700 ± 10	1050 ± 20	3.2 ± 1.5	–	
15-5 PH	H900	Long.	1297 ± 1.0	1450 ± 2.1	12.5 ± 1.1	–	[486]
17-4 PH	Wrought, solution annealed and aged		992	1018	13.4	430	[680]

σ_y = Yield strength, σ_{uts} = Ultimate tensile strength, HV = Vickers hardness.

This activity has received funding from the European Institute of Innovation and Technology (EIT), a body of the European Union, under the Horizon 2020, the EU Framework Programme for Research and Innovation

Table 4.3 – Tensile properties of type 18Ni300 maraging steels fabricated by LPBF [7]

Source	condition	E (GPa)	$R_{p0.2}$ (MPa)	YS (MPa)	UTS (MPa)	elongation at fracture (%)	Hardness (HV or HRC)
[120,123,126,131]	Wrought SA	180		760–895	830–1170	6–17	30-37 HRC
	Wrought AH	183–193		1790–2070	1830–2100	5–11	525 HV/54 HRC
[119]	L-PBF AP				1178	7.9	381 HV
	L-PBF SA				1080	10.2	341 HV
	L-PBF AH				2164	2.5	645 HV
[123]	L-PBF AP	181		815–1080	1010–1205	8.3–12	420 HV
	L-PBF SA	161		800	950	13,5	320 HV
	L-PBF AH	220		1750	1850	5,1	600 HV
[124]	L-PBF AP						370 HV
	L-PBF AH						573 HV
[121]	L-PBF AP		1000		1200	8	
[125]	L-PBF AP		900		1200	6	
	L-PBF AH		1950		2000	1,5	630 HV
[126]	L-PBF AP				1085–1192	5–8	30-35 HRC
[127]	L-PBF AP	166		985	1152	7.6	34 HRC
[129]	L-PBF AP			915	1188	6.1	371 HV
	L-PBF SA						279 HV
	L-PBF AH			1957	2017	1.5	600 HV
[131]	L-PBF AP	163	1214		1290	13,3	40 HRC
	L-PBF AH	189	1998		2217	1,6	58 HRC
[120]	L-PBF AP			915	1165	12.4	35-36 HRC
	L-PBF AH			1967	2014	3.3	53-55 HRC
	L-PBF SA			962	1025	14.4	28-29 HRC
	L-PBF SA + AH			1882	1943	5.6	52-54 HRC

Table 4.4 – Tensile properties of structural and tool steels fabricated by LPBF [6]

Ferrous alloy	Process	UTS (MPa)	YS (MPa)	EL (%)
Iron (electrolytic, annealed) [201]	Wrought	240–280	70–140	40–60
Iron (0.004%C) [202]	LPB	450	380	20
Iron (0.02%C) [37]	LPB	350–410	240–300	10
AISI 1005 [203]	LPB	305	164	–
AISI 1033 [34]	LPB	–	650[a]	–
AISI 1050 [34]	LPB	–	800[a]	–
AISI 1075 [34]	LPB	–	1150[a]	–
4130 – as built [149]	LPB	1503 ± 69	1344 ± 67	12 ± 2
17-4 PH SS ASTM A564 [125]	Wrought (ST + PA)	1310	1170	10
17-4 PH SS [136]	LPB	1255 ± 3	661 ± 24	16.2 ± 2.5
304 SS [204]	LPB (orthogonal to building direction)	715.5 ± 1.5	568 ± 2	41.7 ± 1.1
304 [205]	LPF longitudinal	710	448	59
	LPF transverse	324	655	70
18Ni-300 M [77]	Wrought	1000–1170	760–895	6–15
18Ni-300 M [77]	LPB	1290 ± 114	1214 ± 99	13.3 ± 1.9
18Ni-300 M [142]	LPB	1165 ± 7	915 ± 7	12.44 ± 0.14
4340 [53] 593 °C stress-relieved	LPB	1289–1310	1365	16–17
HY100 [39] as per MIL-S-16216	Wrought	Not specified	690–827	>18%
HY100 – as built (xy) [39]	LPB	1200 ± 15	1160 ± 15	6 ± 2
HY100 [39] direct temper 650 °C-2 h-AC (xy)	LPB	880 ± 10	710 ± 30	8 ± 3
HY100 [39] 900 °C-1 h-WQ + 650 °C-2 h-AC	LPB	780 ± 10	690 ± 10	18 ± 2
H13 [206]	LPB	1000–1200	–	0.9–1.9
H13 [207]	LPB	1370 ± 175.1	1003.0 ± 8.5	1.7 ± 0.6
M2 – heat treated [36]	Wrought	1611	–	1.3
M2 [36]	LPB	1286	–	0.6

[a] Compressive, ST: solution treated, PA: peak aged.

4.2. References

1. M. Abdelwahed, R. Casati, S. Bengtsson, A. Larsson, M. Riccio, M. Vedani. Effects of Powder Atomisation on Microstructural and Mechanical Behaviour of L-PBF Processed Steels. Metals, 10 (2020) 1474

This activity has received funding from the European Institute of Innovation and Technology (EIT), a body of the European Union, under the Horizon 2020, the EU Framework Programme for Research and Innovation

2. M. Abdelwahed, S. Bengtsson, R. Casati, A. Larsson, S. Petrella, M. Vedani. Effect of water atomization on properties of type 4130 steel processed by L-PBF. Submitted for publication to Materials and Design (2021)
3. T. Fedina, J. Sundqvist, A.F.H. Kaplan. Spattering and oxidation phenomena during recycling of low alloy steel powder in Laser Powder Bed Fusion. Materials Today Communications, 27 (2021) 102241
4. T. Fedina, J. Sundqvist, J. Powell, A.F.H. Kaplan. A comparative study of water and gas atomized low alloy steel powders for additive manufacturing. Additive Manufacturing, 36 (2020) 101675
5. N. Haghdadi, M. Laleh, M. Moyle, S. Primig. Additive manufacturing of steels: a review of achievements and challenges. Journal of Materials Science, 56 (2021) 64–107
6. H. Fayazfar, M. Salarian , A.Rogalsky , D. Sarker, P. Russo, V. Paserin, E. Toyserkani. A critical review of powder-based additive manufacturing of ferrous alloys: Process parameters, microstructure and mechanical properties. Materials and Design, 144 (2018) 98-128
7. P. Bajaj, A. Hariharan, A. Kini, P. Kürnsteiner, D. Raabe, E.A. Jagle. Steels in additive manufacturing: A review of their microstructure and properties. Materials Science & Engineering A, 772 (2020) 138633
8. S. Gorsse, C. Hutchinson, M. Gouné, R. Banerjee. Additive manufacturing of metals: a brief review of the characteristic microstructures and properties of steels, Ti-6Al-4V and high-entropy alloys. Science and Technology of Advanced Materials, 18 (2017) 584–610
9. T. DebRoy, H.L. Wei, J.S. Zuback, T. Mukherjee, J.W. Elmer, J.O. Milewski, A.M. Beese, A. Wilson-Heid, A. De, W.Zhang. Additive manufacturing of metallic components – Process, structure and properties. Progress in Materials Science, 92 (2018) 112-224

This activity has received funding from the European Institute of Innovation and Technology (EIT), a body of the European Union, under the Horizon 2020, the EU Framework Programme for Research and Innovation